Experimental Study of Highly Excited $^1\Sigma_g^+$ and $^1\Pi_g$ States of the Cesium Dimer

B. A. Rowe[1], J. T. Stahovich[1], S. Magnier[2], V. B. Sovkov[3,4], A. B. Nikolov[1], A. D. Hersh[1], P. L. Wardach[1], J. D. Keen[1], A. M. Lyyra[1], and E. H. Ahmed[1].

[1]Physics Department, Temple University, Philadelphia, PA 19122, USA
[2]Universite Lille, CNRS, UMR8523-PhLAM-Laboratoire de Physique des Lasers, Atomes et Molecules, F-59000 Lille, France
[3]St. Petersburg State University, 7/9 Universitetskaya naberezhnaya, St. Petersburg 199034, Russia
[4]State Key Laboratory of Quantum Optics and Quantum Optics Devices, Institute of Laser Spectroscopy,
College of Physics and Electronics, Shanxi University, Taiyuan 030006, China

Abstract

We report the results of an experimental study on the highly excited $11\,^1\Sigma_g^+$ and $6\,^1\Pi_g$ electronic states of the cesium-133 dimer. The rovibrational structure of these states was probed using the optical-optical double resonance (OODR) technique in which $^{133}Cs_2$ molecules from thermally populated levels in the $X\,^1\Sigma_g^+$ ground state were excited through intermediate levels in either the $B\,^1\Pi_u$ state or the mixed $A\,^1\Sigma_u^+\sim b\,^3\Pi_u$ manifold. Probe laser resonance frequencies were determined by detecting laser induced fluorescence (LIF) from the target states to the ground $a\,^3\Sigma_u^+$ triplet state. The observed states were identified as $^1\Sigma_g^+$ and $^1\Pi_g$ electronic states based on the selection rules for dipole allowed transitions followed by the line patterns in the recorded excitation spectra. Bound-bound fluorescence spectra from rovibrational levels in the target states down to the A $\sim$ b manifold were also taken to further confirm electronic state multiplicity. Two sets of Dunham coefficients corresponding to the two target states were fitted from experimentally determined term values and are reported in the present work. Potential energy curves constructed from these Dunham coefficients are also presented and compared to *ab initio* curves from our collaborators.
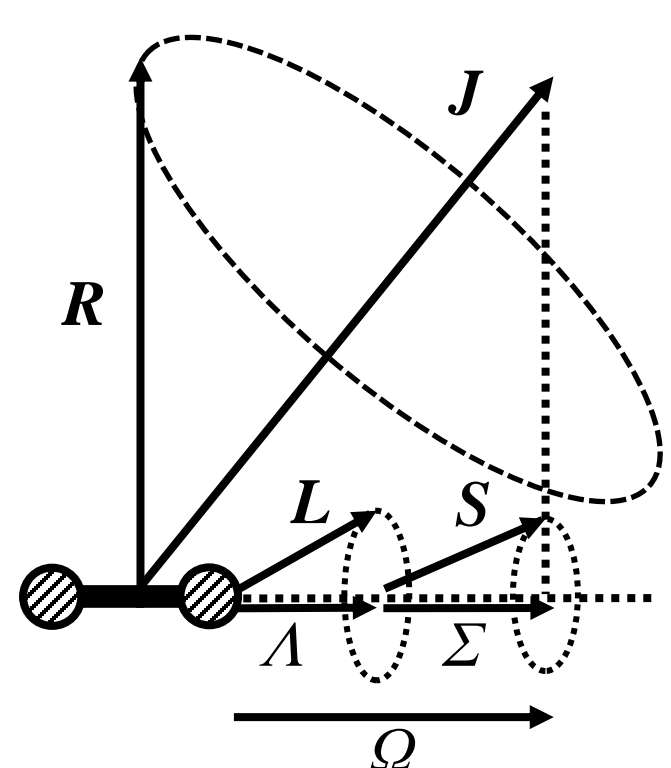
Excitation Scheme
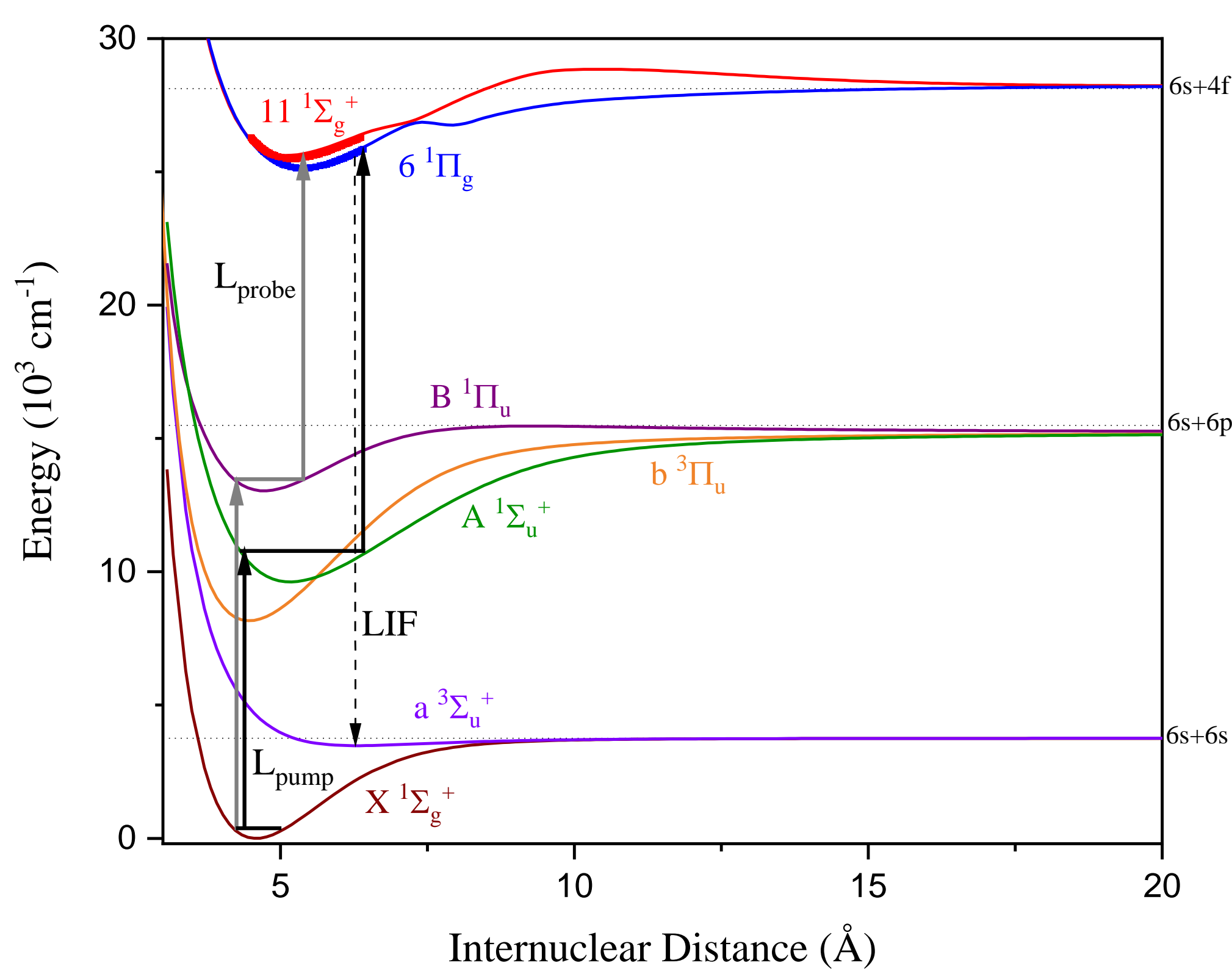
Experimental Setup
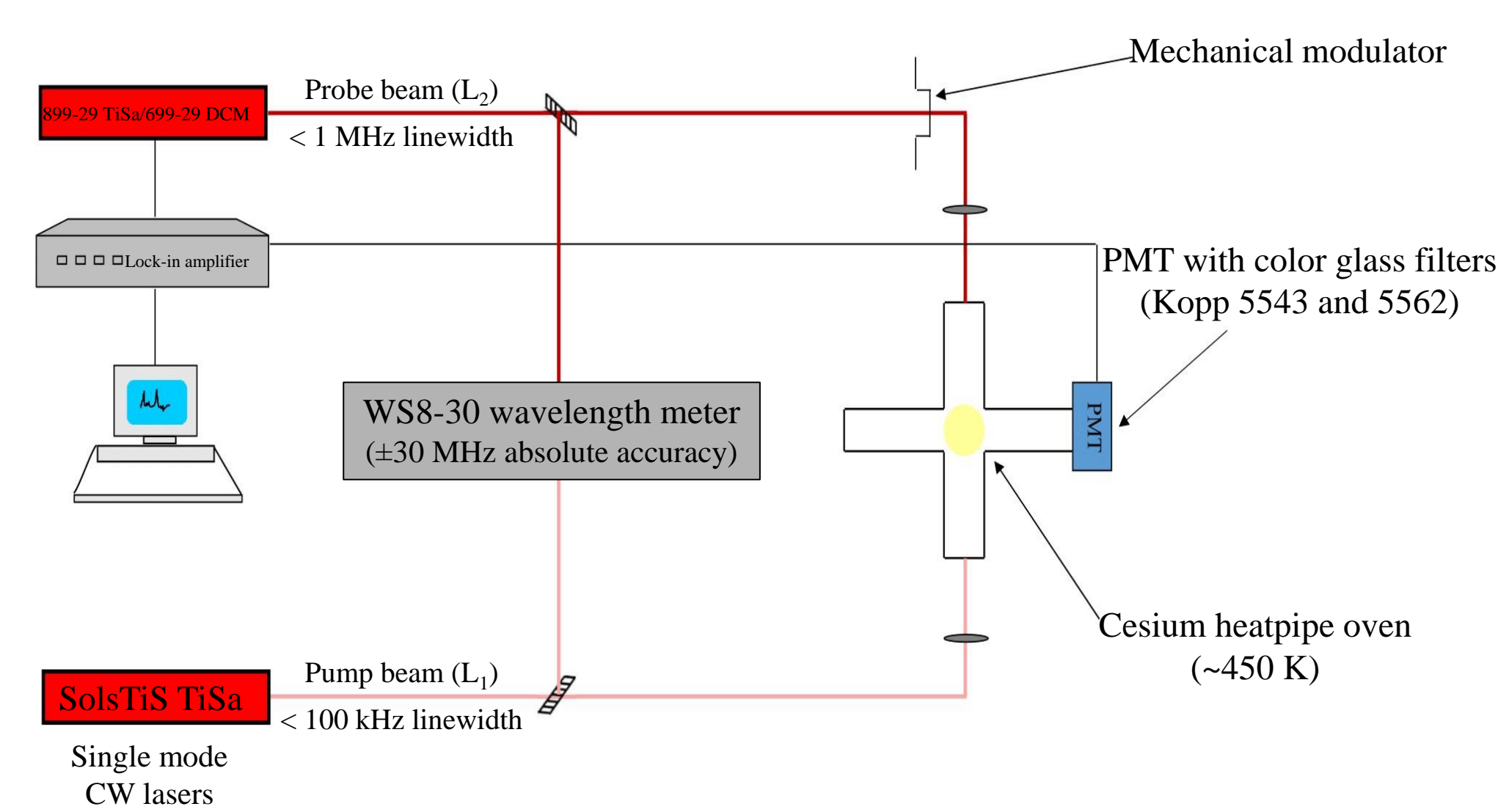
Angular Momenta, Parity, and Selection Rules

Angular momentum coupling scheme for Hund's case (a):

Angular Momenta:
L: electronic orbital angular momentum
Λ: magnitude of projection of L across internuclear axis
R: nuclear rotational angular momentum
S: electronic spin
Σ: magnitude of projection of S across internuclear axis
$\Omega = |\Lambda + \Sigma|$: total angular momentum projection across internuclear axis
$J = R + L + S$: total angular momentum excluding nuclear spin

Parity:
g/u: electronic wavefunction inversion symmetry
$+/-$: electronic wavefunction reflection symmetry
e/f: rotationless total rovibronic wavefunction parity

Selection rules for rovibronic transitions derived by evaluating transition dipole moment matrix elements:

$$M_{\alpha\beta} = \langle n_\alpha \Lambda_\alpha S_\alpha \Sigma_\alpha | \langle v_\alpha | \langle \Omega_\alpha J_\alpha M_\alpha | \boldsymbol{\mu_z} | \Omega_\beta J_\beta M_\beta \rangle |v_\beta\rangle |n_\beta \Lambda_\beta S_\beta \Sigma_\beta\rangle$$

$$= \int d\tau_e\, \psi_{\alpha,e}^* \, \boldsymbol{\mu_{z,e}} \, \psi_{\beta,e} \int dr\, \psi_{\alpha,v}^* \, \psi_{\beta,v} \int d\theta\, d\varphi \sin\theta \cos\theta\, \psi_{\alpha,r}^* \, \psi_{\beta,r}$$

Where $\psi_{e/v/r}$ is the electronic/vibrational/rotational component of the total molecular wavefunction, respectively. Dipole transition selection rules are tabulated below:

- $\Delta\Lambda = 0, \pm 1$
- $\Delta S = 0$
- $g \leftrightarrow u$
- $+ \leftrightarrow +,\ -\leftrightarrow -$ (electronic wavefunction only, need only be specified when $\Lambda = 0$)
- $\Delta J = -1, 0, 1$ ("P branch", "Q branch", "R branch")
  - When $\Lambda' = \Lambda'' = 0$, $\Delta J = \pm 1$ ONLY.
  - $\Delta J = 0$ transition tends to be weak/nonexistent when $\Delta\Lambda = 0$ and J is large
- $e \leftrightarrow e,\ f \leftrightarrow f$ for P/R branches, $e \leftrightarrow f$ for Q branches
  - Note: All rotational levels in $^1\Sigma^+$ states have e parity ONLY, whereas levels in $^1\Pi$ states and above come in degenerate e/f pairs.
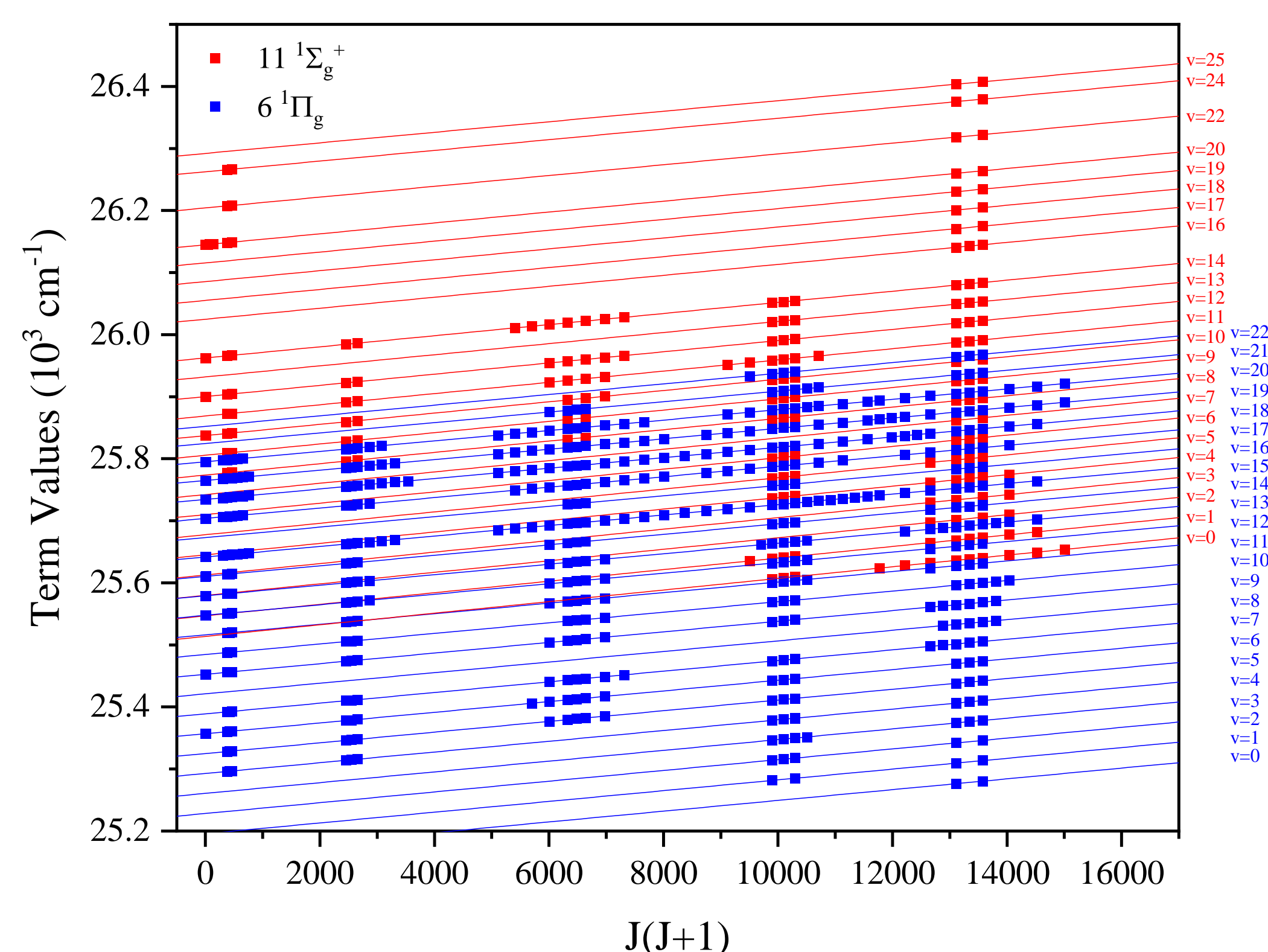
Example Excitation Spectra
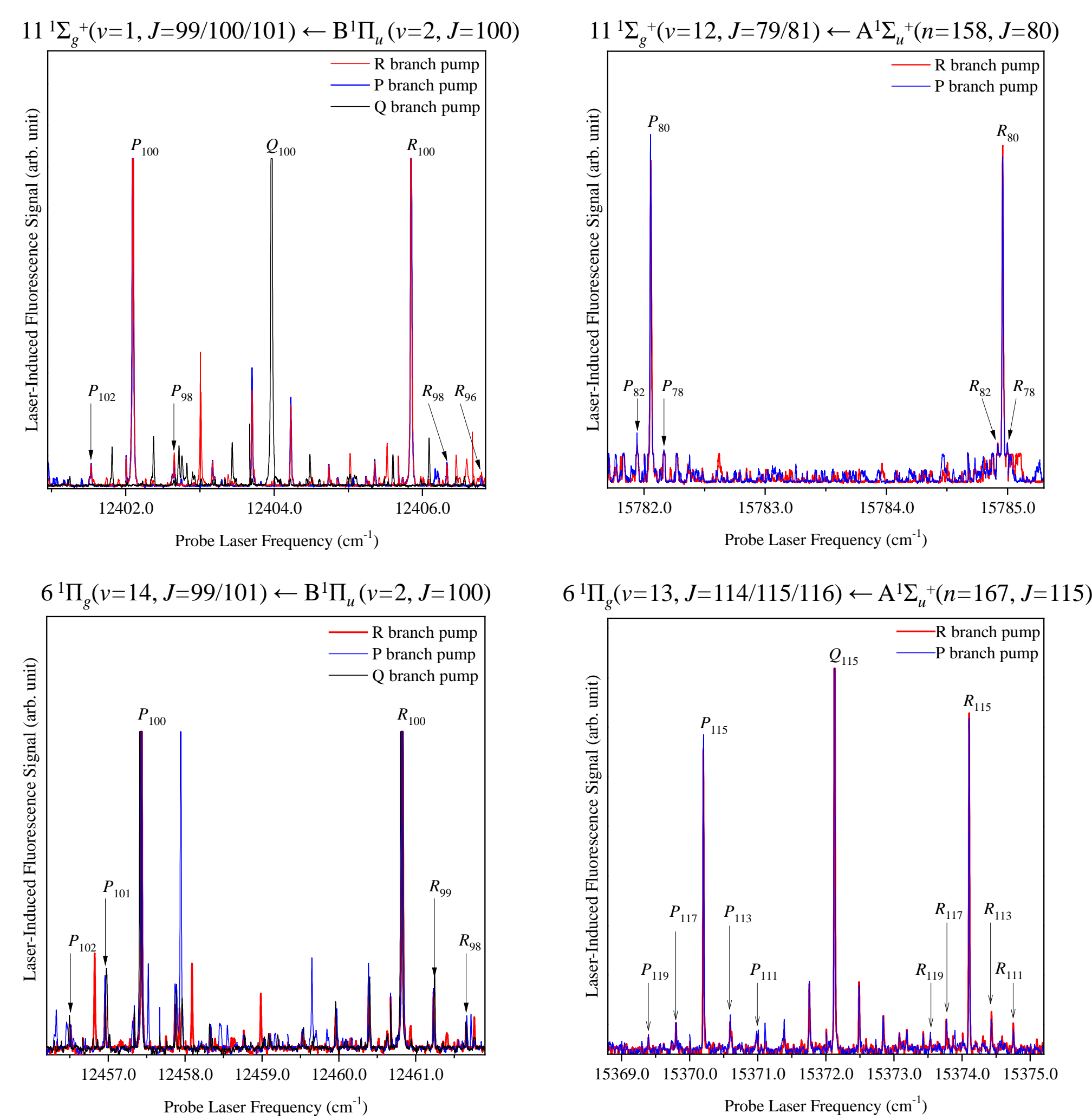
Bound-Bound Fluorescence Spectra
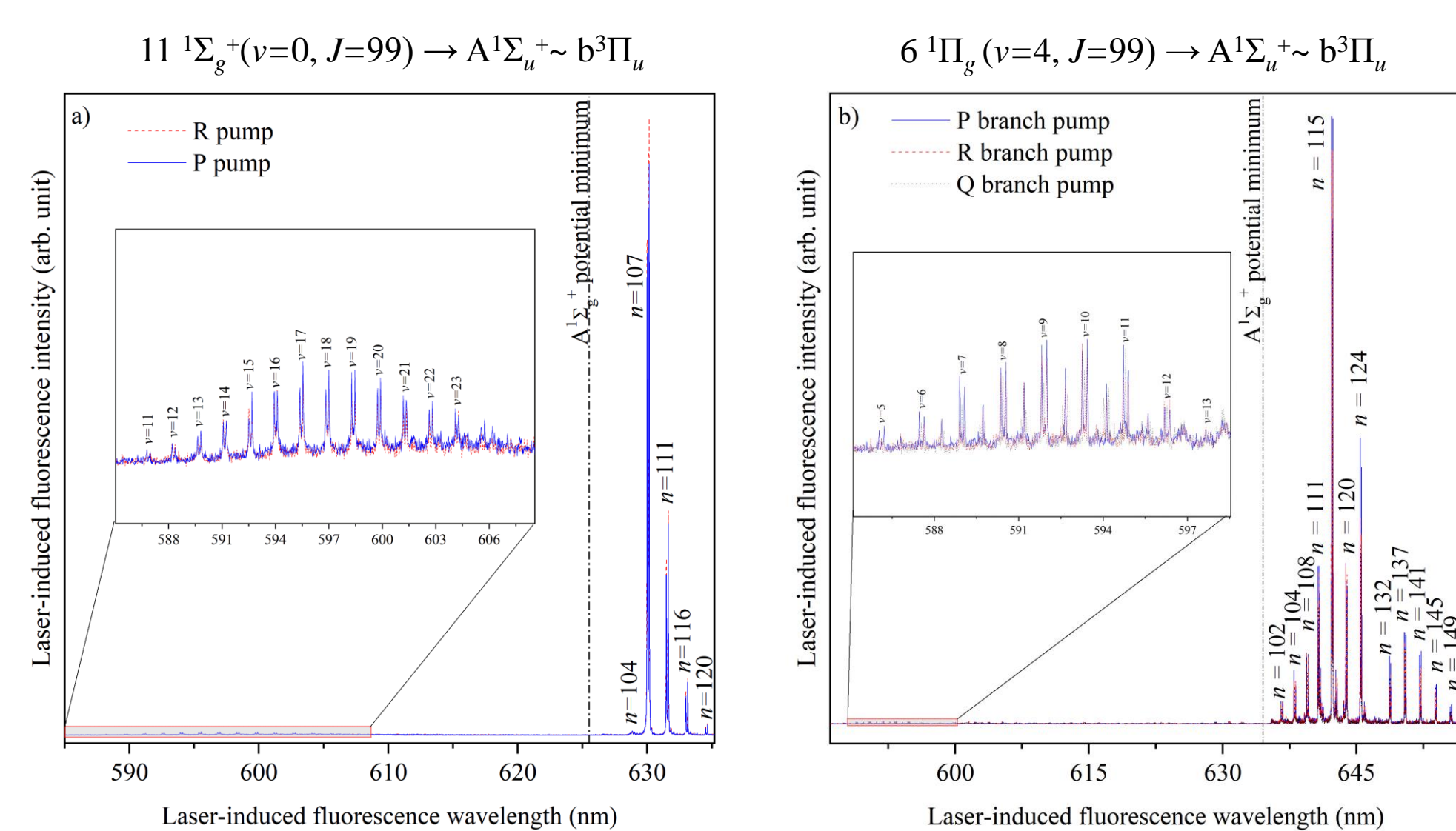
Fluorescence to levels with predominately singlet character in the mixed $A\,^1\Sigma_u^+\sim b\,^3\Pi_u$ manifold ~1000x stronger than that of predominately triplet character levels.

Term Values

References

1. G. Herzberg, Spectra of Diatomic Molecules (Van Nostrand, New York, 1950).
2. P. F. Bernath, Spectra of Atoms and Molecules (Oxford University Press, New York, 1995).
3. J. M. Bai et al., Global analysis of data on the spin-orbit-coupled $A\,^1\Sigma_u^+$ and $b\,^3\Pi_u$ states of Cs_2, Physical Review A **83** (2011).
4. J. L. Dunham, The energy levels of a rotating vibrator, Physical Review **41**, 721 (1932).
5. R. J. Le Roy, RKR1 2.0: A Computer Program Implementing the First-Order RKR Method for Determining Diatomic Molecule Potential Energy Curves, University of Waterloo Chemical Physics Research Report CP-657R (2004).

Dunham Fitting and RKR Results

The total energy of a diatomic molecule can be decomposed into three distinct terms:

$$E_{total} = E_{el} + E_{vib} + E_{rot} = T_e + G(v) + F_v(J).$$

The electronic energy term T_e sets the position of the potential well minimum for a given electronic state.

The vibrational and rotational terms $G(v)$ and $F_v(J)$ produce the energy levels associated with a vibrating rotor potential and can be expanded into the following power series:

$$G(v) = \omega_e\left(v+\frac{1}{2}\right) - \omega_e x_e\left(v+\frac{1}{2}\right)^2 + \omega_e y_e\left(v+\frac{1}{2}\right)^3 + \cdots$$

and

$$F_v(J) = B(v)\,J\,(J+1) - D(v)\,J^2\,(J+1)^2 + \cdots.$$

The leading term of the $G(v)$ expansion generates the energy levels corresponding to a harmonic oscillator potential, while subsequent higher order terms alter said levels to account for the anharmonicity of the actual physical potential.

The rotational coefficient $B(v)$ and the centrifugal distortion coefficient $D(v)$ of the $F_v(J)$ expansion can be further expanded still:

$$B(v) = B_e - \alpha_e\left(v+\frac{1}{2}\right) + \gamma_e\left(v+\frac{1}{2}\right)^2 + \cdots$$

and

$$D(v) = D_e + \beta_e\left(v+\frac{1}{2}\right) + \cdots.$$

These four series can be neatly summarized into one all-encompassing expansion, known as a "Dunham expansion", given by:

$$T_{v,J} = \sum_{k,l} Y_{k,l}\,\left(v+\frac{1}{2}\right)^k\,[j(j+1)-\Lambda^2]^l,$$

Where the coefficients $Y_{k,l}$ relate to the previously given spectroscopic coefficients by:

$Y_{10} \approx \omega_e$	$Y_{20} \approx -\omega_e x_e$	$Y_{30} \approx \omega_e y_e$
$Y_{01} \approx B_e$	$Y_{11} \approx -\alpha_e$	$Y_{21} \approx \gamma_e$
$Y_{02} \approx -D_e$	$Y_{12} \approx -\beta_e$	etc.

The Dunham coefficients of our target states, calculated via a least squares fitting procedure from found term values, were determined to be:

State	$T_e + Y_{00}$	$Y_{10}(\omega_e)$	$Y_{20}(-\omega_e x_e)$	$Y_{30}(\omega_e y_e)$	$Y_{40}(\omega_e z_e)$
$11\,^1\Sigma_g^+$	25496.5018(229)	33.28830(544)	$-7.8307(921)\times 10^{-2}$	$-4.9450(9041)\times 10^{-4}$	$4.4178(4113)\times 10^{-5}$
$6\,^1\Pi_g\ e$	25146.9142(2889)	32.50844(29732)	$0.319694(86980)$	$-9.45641(151248)\times 10^{-2}$	$1.2074862(1458082)\times 10^{-2}$
$6\,^1\Pi_g\ f$	25146.4905(2779)	32.05255(25341)	$0.258184(133295)$	$-0.130725(332948)$	$2.6117630(5138468)\times 10^{-2}$
State	$Y_{01}(B_e)$	$Y_{11}(-\alpha_e)$	$Y_{21}(\gamma_e)$	Y_{31}	$Y_{02}(-D_e)$
$11\,^1\Sigma_g^+$	$9.44898(195)\times 10^{-3}$	$-3.5330(349)\times 10^{-5}$	$6.254(284)\times 10^{-7}$	$-2.0281(713)\times 10^{-8}$	$-3.407(54)\times 10^{-9}$
$6\,^1\Pi_g\ e$	$8.63825(2183)\times 10^{-3}$	$1.30526(19162)\times 10^{-4}$	$-5.59740(66535)\times 10^{-5}$	$1.032241(117249)\times 10^{-5}$	$-2.874(72)\times 10^{-9}$
$6\,^1\Pi_g\ f$	$8.68724(1991)\times 10^{-3}$	$5.0752(17975)\times 10^{-5}$	$-2.53727(63545)\times 10^{-5}$	$4.71660(113030)\times 10^{-6}$	$-6.30(111)\times 10^{-10}$

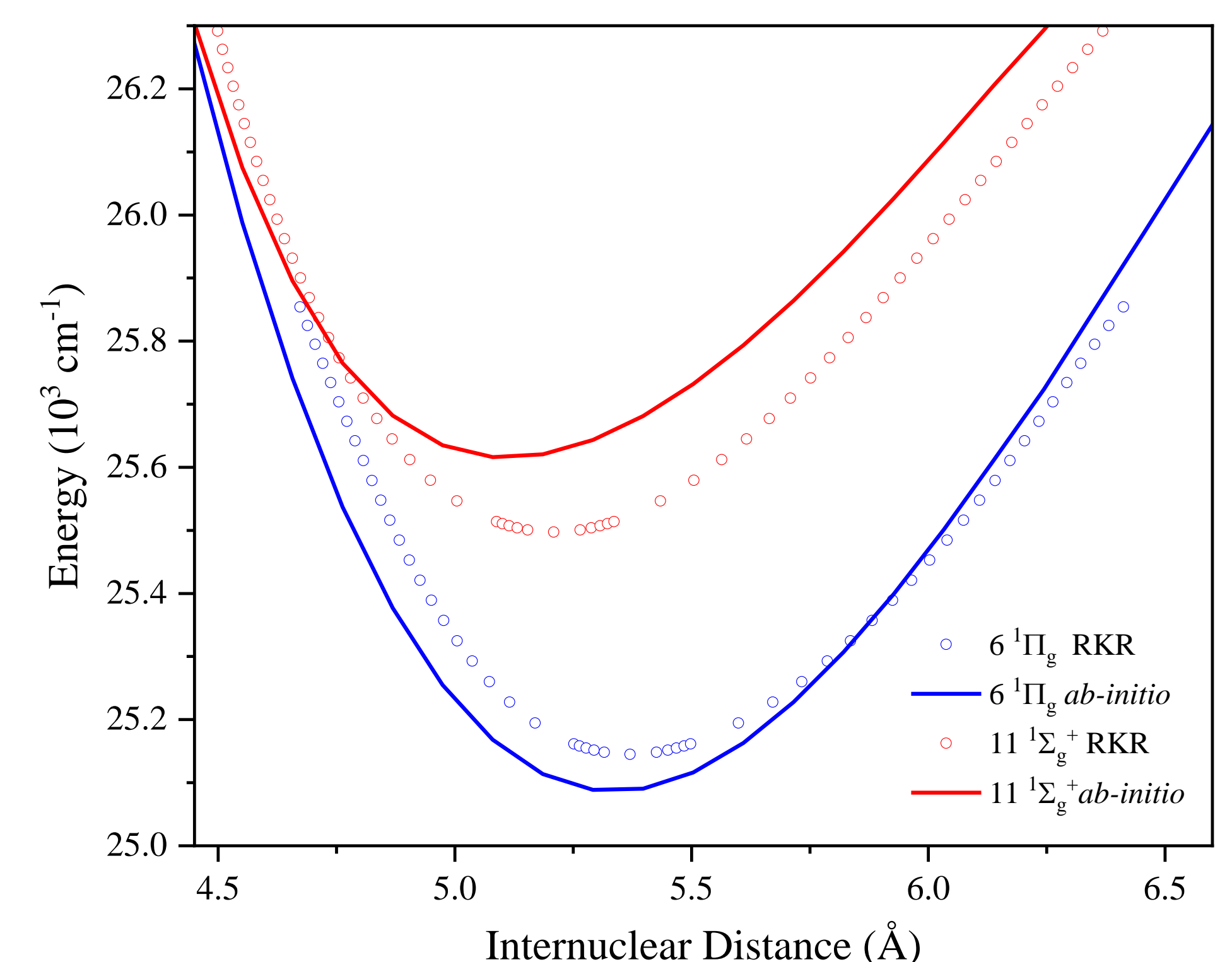*Fitted Dunham coefficients for the reported states. All values given in units of cm^{-1}.*

Potential energy curves can be generated from Dunham coefficients via the Rydberg-Klein-Rees (RKR) method. This method provides a means of numerically calculating the turning points of the PE curve for a given state by iteratively solving the following Klein integrals:

$$R_+ - R_- = C \int_{v_{min}}^{v} \frac{dv'}{[G_v - G_{v'}]^{1/2}}$$

and

$$\frac{1}{R_-} - \frac{1}{R_+} = C \int_{v_{min}}^{v} \frac{B_{v'}\,dv'}{[G_v - G_{v'}]^{1/2}}$$

where $C = \left(\frac{2\hbar}{\mu}\right)^{1/2}$. Via this process, the following RKR curves for our target states were produced:

Support